DYNAMICAL ANALYSIS OF AN ATOMIC FORCE MICROSCOPY (AFM) INCLUDING FRACTIONAL-ORDER

Angelo Marcelo Tusset, a.m.tusset@gmail.com[1]
Frederic Conrad Janzen, fcjanzen@utfpr.edu.br[1]
Vinícius Piccirillo, piccirillo@utfpr.edu.br[1]
Jose Manoel Balthazar, jmbaltha@gmail.com[2]
Rodrigo Tumolin Rocha, digao.rocha@gmail.com[3]

[1]UTFPR, Av. Monteiro Lobato, s/n, km 04 - CEP 84016-210 - Ponta Grossa – PR, Brazil
[2]UNESP-ITA, Praça M.al Eduardo Gomes, 50 - Vila das Acácias. CEP 12.228-900-São José dos Campos – SP, Brazil
[3]UNESP, Av. Eng. Luiz Edmundo C. Coube, 14-01, Vargem limpa, 17033-360, Bauru – SP, Brazil

Abstract: *In this work, the nonlinear dynamics of an Atomic Force Microscope micro cantilever operating in tapping mode is investigated, considering the influence of damping, nonlinear stiffness term, and squeeze film damping in fractional-order. The response analysis of the system is carried out by bifurcation diagrams, phase portraits and Lyapunov exponents. Numerical results showed that the analyzed parameters play an important role because they can lead to different responses, like periodic and chaotic motion. In particular, for squeeze film damping in fractional-order, the results showed the influence of the order of the derivative on the dynamic (regular or non-periodic) behavior. To characterize these behaviors the 0-1 test was used once this is a good tool to characterize fractional-order differential systems.*

Keywords: *Atomic Force Microscopy, Tapping Mode Vibration, Chaos, Fractional-Order, 0-1 Test.*

1. INTRODUCTION

A typical (AFM) system consists of a micro-machined cantilever probe and a sharp tip mounted to a Piezoelectric (PZT) actuator and a position sensitive photo detector for receiving a laser beam reflected off the end-point of the beam to provide cantilever deflection feedback as show Fig. 1 (Jalili and Laxminarayana, 2004).

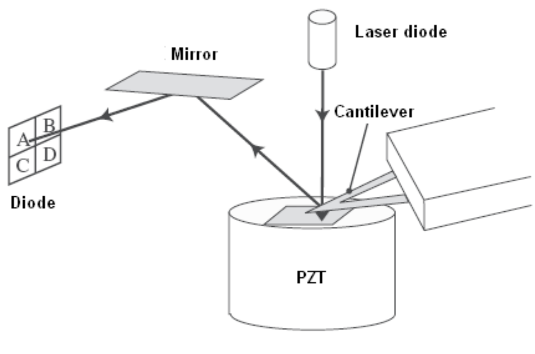

Figure 1. Schematic diagram of the atomic force microscope (Frétigny, 2007).

According to Balthazar et al. (2014) that the nonlinear dynamic atomic force microscopy, in essence, consists of a vibrating micro cantilever, with a nanoscale tip, which interacts with a sample surface via short and long range intermolecular forces.

According to Garcia and Pérez (2003), Giessibl (2003), Rodrigues et al. (2014); Nozaki et al. (2013), Balthazar et al. (2012a), (2012b), the main interest in the nonlinear dynamics of AFM grew out of observations of instabilities, which occur at certain oscillation amplitudes. Then, it has been required to develop a new generation of AFM. In addition, according to Burgess and Daniel (2006) the micro-cantilever of AFM in tapping mode may exhibits chaotic behavior under certain conditions. This subject has been experimentally observed. The existence of chaotic behavior in AFM is highly undesirable because of its bad effects on the system once this type of complex irregular motion causes the AFM to give inaccurate measurements and low resolution of the achieved sample topography.

Accordingly, to ensure good performance of the microscope is necessary to know the AFM operating conditions to a region of the parameter space (Basso and Bagni, 2004).

Considering the importance of the knowledge of the dynamics of the AFM system for parametric variation, this work presents the numerical results of the analysis of the influence of damping, nonlinear stiffness term, and squeeze film damping in fractional-order, in the dynamic of the system AFM in tapping mode.

This paper is organized as follows. In Section 2 is presented the mathematical modelling. In Section 3, the proposed control is designed and implemented, and the parameters: damping, nonlinear stiffness term of the beam, were numerical analyzed considering bifurcation diagrams and Lyapunov exponent. Section 4 presents the numerical analysis of the squeeze film damping in fractional-order considering time history of the displacement of the tip of the beam, phase plane, Poincare map and 0-1 test. The conclusions are shown in Section 5.

2. MATHEMATICAL MODEL FOR A TYPICAL AFM WITH A NONLINEAR BEHAVIOR

Figure 2a presents the physical model of the tapping mode AFM. The basis of the cantilever is excited by a piezo-electric actuator, with the displacement given by a harmonic force, and in Fig. 2b, is presented the cantilever as a mass-spring-damper system vibrating closely to the surface of the sample.

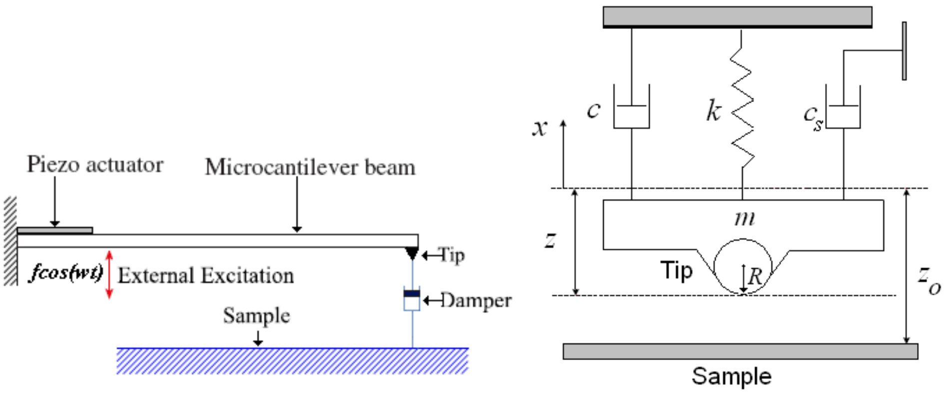

(a) **(b)**

Figure 2. Model of an AFM (Balthazar et al., 2014).

The tip is taken as a sphere of radius R and the distance between the sample and the cantilever by Z_0 (distance between an equilibrium position of the cantilever and the sample), when only the gravity force acts on it. The position of the cantilever is given by x, measured from the equilibrium position (Balthazar et al., 2014).

According to Rutzel et al. (2003) the interaction between the tip of the cantilever and the surface of the sample, may be modeled as being the interaction between a sphere and a plane surface, as in Eq. (1).

$$U(x, z_0) = \frac{A_1 R}{1260(z_0 + x)^7} - \frac{A_2 R}{6(z_0 + x)} \tag{1}$$

where: $U(x,z_0)$ is the Lennard-Jones (LJ) potential, A_1 is the Hamaker constant to the attractive potential and A_2 is the constant of Hamaker to the repulsive potential.

The forces can be represented by the sum of attractive and repulsive forces, expressed them in Eq. (2), by Rutzel et al. (2003):

$$F = -\frac{\partial U}{\partial(x + z_0)} = \frac{A_1 R}{180(z_0 + x)^8} - \frac{A_2 R}{6(z_0 + x)^2} \tag{2}$$

Note that during the process of the tapping mode of AFM, the cantilever is also excited by a harmonic force $f\cos(wt)$, and the contact tip-sample generates the force.

The governing equation of the motion of the cantilever can be determined, in given in Eq. (3).

$$m\ddot{x} = F_k + F_c + F_{c_s} + F + f\cos wt \tag{3}$$

where: x is the displacement of the tip of the cantilever, considering the equilibrium position in the absence of the external forces, the mass of the cantilever is represented by m, the forces F can be represented by the sum of attractive and repulsive forces, expressed by Eq. (2), the conservative force of the spring is F_k, F_c the damping force of the elastic term is F_c, and the squeeze film damping is given by F_{cs}. In addition, the spring stiffness also is a parameter, which can be affected by elastic term phenomena and nonlinearities. Therefore, the variation of the conservative force of the spring (F_k) can be represented by (Balthazar et al., 2014):

$$F_k = k_l x + k_{nl} x^3 \tag{4}$$

The dissipation force F_c can be obtained from (Balthazar et al., 2014):

$$F_c = c\dot{x} \tag{5}$$

According to Zhang et al. (2009) the F_{cs} squeeze film damping is represent by:

$$F_{c_s} = c_s \dot{x} = \frac{\mu_{eff}\,\beta^3 l}{(x+z_0)^3}\dot{x} \tag{6}$$

where μ_{eff} is the effective viscous coefficient, the width of the cantilever is β and its length as l.

The equation of motion (3) will become:

$$m\ddot{x} + c\dot{x} + k_l x + k_{nl}x^3 = \frac{A_1 R}{180(z_0+x)^8} - \frac{A_2 R}{6(z_0+x)^2} + \frac{\mu_{eff}\,\beta^3 l}{(x+z_0)^3}\dot{x} + f\cos wt \tag{7}$$

The equation (7) can be represented in following dimensionless form:

$$\begin{aligned}\dot{x}_1 &= x_2\\ \dot{x}_2 &= -rx_2 - bx_1 - cx_1{}^3 - \frac{d}{(a+x_1)^2} + \frac{e}{(a+x_1)^8} + g\cos\Omega\tau - \frac{p}{(a+x_1)^3}x_2\end{aligned} \tag{8}$$

where: $x_1 = y$, $x_2 = \dot{y}$, $\tau = w_1 t$, $y = \frac{x}{z_s}$, $\dot{y} = \frac{\dot{x}}{w_1 z_s}$, $a = \frac{z_0}{z_s}$, $b = \frac{k_l}{k_{at}}$, $c = \frac{k_{nl}}{k_{at}} z_s^2$, $d = \frac{4}{27}$, $e = \frac{2}{405}\left(\frac{a}{z_s}\right)^6$, $g = \frac{f_0}{k_{at} z_s}$, $p = \frac{\mu_{eff}\,\beta^3 l}{m w_1 z_s^3}$, $\Omega = \frac{w}{w_1}$, $r = \frac{1}{Q}$ and $Z_s = \left(\frac{2}{3}\right)\left(\frac{A_2 R}{3k_l}\right)^{1/3}$.

3. NUMERICAL SIMULATIONS, RESULTS AND DISCUSSIONS FOR A TYPICAL AFM

Considering the variation of the nonlinear term of the spring stiffness (c) in the behavior of the nonlinear AFM model as $c \in [0.28, 0.38]$, and $a = 1.6$, $b = 0.05$, $c = 0.35$, $d = 4/27$, $\mathrm{e} = 0.0001$, $\mathrm{g} = 0.2$, $\Omega = 1$, $\mathrm{p} = 0.005$ and $r = 0.1$, Figs. 3 show the bifurcation diagram and the Largest Lyapunov exponent for nonlinear term of the spring stiffness (c) variation.

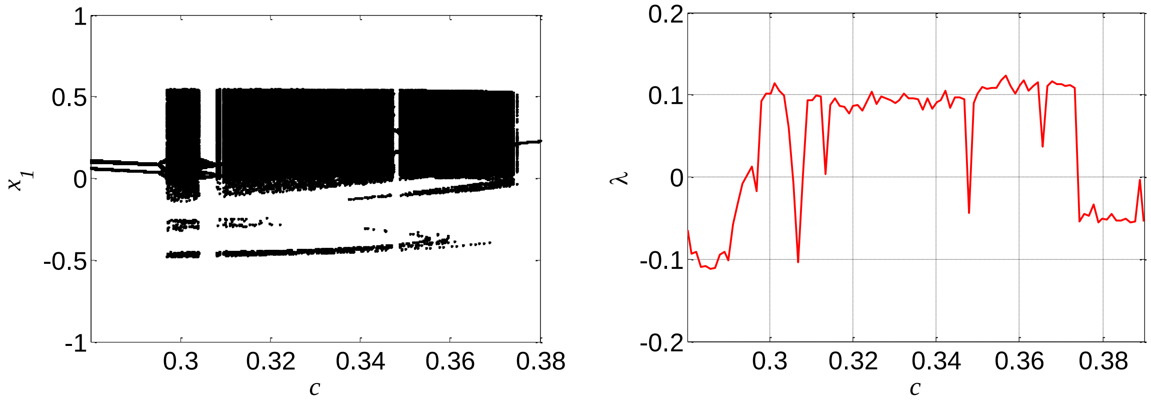

Figure 3. Variation of the nonlinear term of the spring stiffness coefficient $c \in [0.28, 0.38]$. (a) Bifurcation diagram showing maximum displacement. (b) Largest Lyapunov exponent.

It can be observed in Fig. 3, the coefficient *c* has some influence on the dynamical behavior of the beam. It is possible through an appropriate choice of the imposed coefficient a periodic or chaotic behavior of the system.

Next, we will consider the variation of the beam's damping coefficient (*r*) in order to see its influence in the behavior of the nonlinear AFM model, in the interval $r \in [0.05, 0.15]$, and $a = 1.6$, $b = 0.05$, $c = 0.35$, $d = 4/27$, $e = 0.0001$, $g = 0.2$, $\Omega = 1$ and $p = 0.005$.

Figures 4 show the bifurcation diagram and the Largest Lyapunov exponent for the variation of the beam's damping coefficient (*r*). The damping coefficient also interfere on the dynamic of the system, being predominantly with chaotic behavior to $r \in [0.05, 0.135]$ and periodic for $r \in [0.135, 0.15]$.

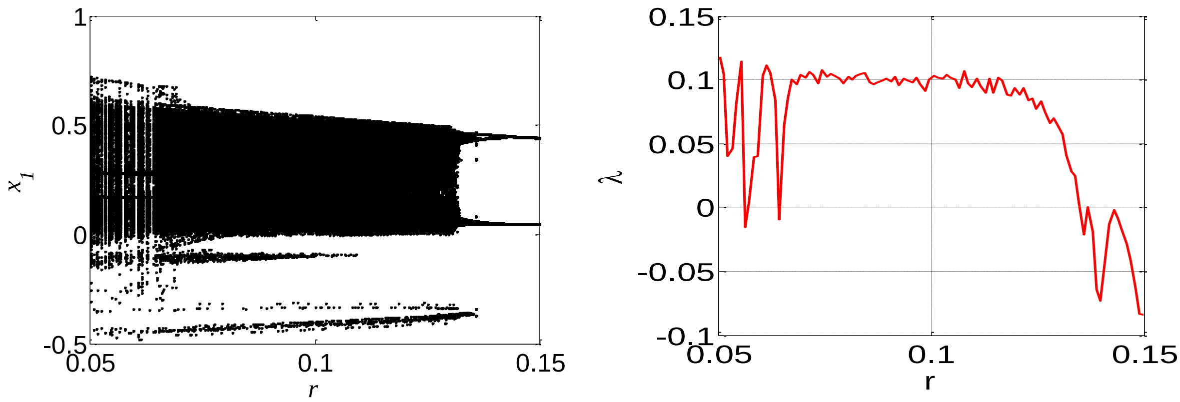

Figure 4. Variation of the damping force of the elastic term coefficient $r \in [0.05, 0.15]$. Bifurcation diagram showing maximum displacement. (b) Largest Lyapunov exponent.

Figure 5 shows the maximum Lyapunov exponent for the variation of the damping force of the elastic term coefficient $r \in [0.05, 0.15]$ and nonlinear term of the spring stiffness coefficient $c \in [0.28, 0.38]$.

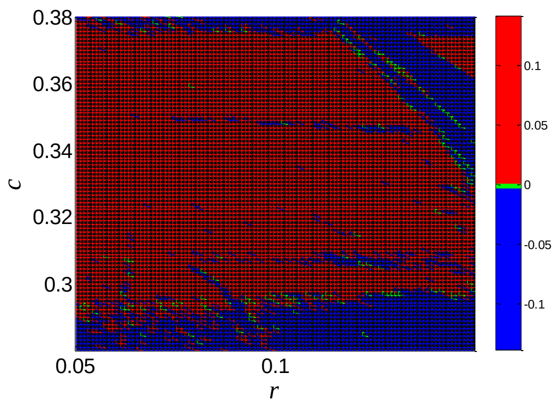

Figure 5. Largest Lyapunov exponent.

Analyzing Fig. 5, it is possible to see that the most influential factor in the chaotic behavior of the system is the nonlinear term of rigidity, demonstrating the importance of the appropriate choice of the beam material and the importance of the nonlinear term in the mathematical model of the AFM.

4. INFLUENCES OF THE SQUEEZE FILM DAMPING IN THE BEHAVIOR OF THE AFM SYSTEM

In this section, we will discuss the influence of the squeeze film damping in the behavior of the AFM system. In Eq. (8) we can observe a dissipation term caused by the squeeze film damping ($-\frac{p}{(a+x_1)^3}x_2$), inherent in the viscous behavior of the sample.

Then, in Fig. 6, the variation of the parameter (*p*) was performed, whose parameter depends on the effective viscous coefficient (μ_{eff}). The parameter *p* has a small influence on chaotic behavior of the system, as the Lyapunov exponent remained positive for practically any change, except for $p = 0.0072$ in the Lyapunov exponent tended to zero.

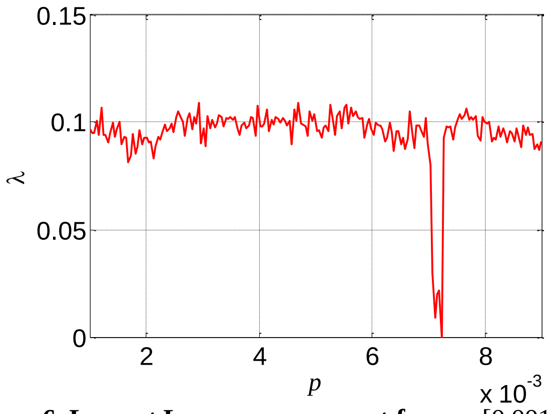

Figure 6. Largest Lyapunov exponent for $p \in [0.001, 0.009]$**.**

Considering the numerical values of the parameters: $\Omega = 1$, $r = 0.1$, $b = 0.05$, $c = 0.35$, $d = 4/27$, $e = 0.0001$, $g = 0.2$, $p = 0.005$, $a = 1.6$, $x_{1_0} = 0$ and $x_{2_0} = 0$. The displacement of the tip is shown in Fig. 7a, phase plane in Fig. 7b and Poincare map in Fig. 7c.

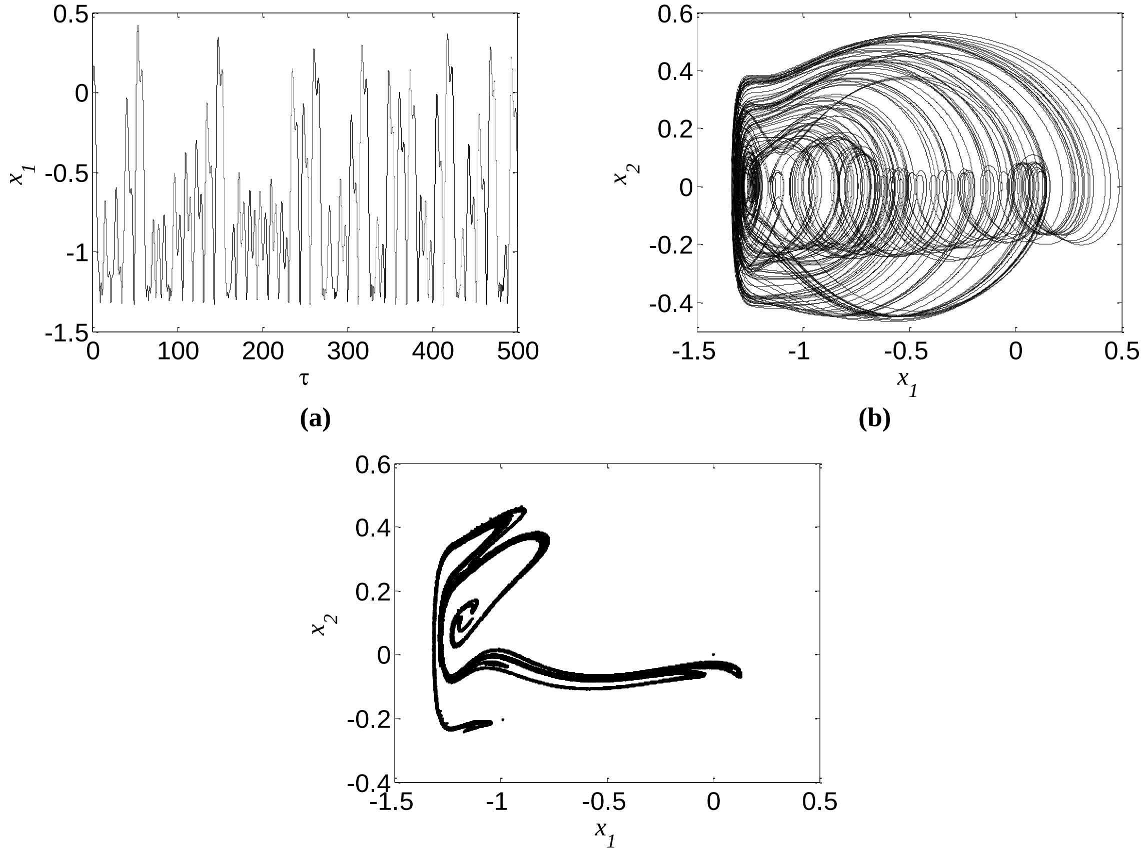

(c)

Figure 7. (a) Displacement of the tip. (b) Phase portrait. (c) Poincare map.

4.1. Chaos Analysis in System with a Fractional-Order

In the case of the sample related to damping, it is possible to see that the behavior is not only viscous but viscoelastic. For the viscoelastic behavior is possible the use of the fractional-order derivatives to analyze the dynamic behavior of the system (Bagley and Calico, 1991). Due to essential differences between ordinary differential equations (ODE) and fractional-order differential equations (FODE). Most of characteristics or conclusions of the ODE systems cannot be directly extended to the case of the FODE systems (Yu et al., 2009).

Differential equations may involve Riemann–Liouville differential operators of fractional-order $q > 0$, which generally takes the form below (Yu et al.,2009):

$$D^{q}x(t)=\frac{1}{\Gamma(\eta-q)}\int_{t_0}^{t}\frac{x^{(\eta)}(u)}{(t-u)^{q-\eta+1}}du \tag{9}$$

where η is the first integer not less than q. It is easily proved that the definition is the usual derivatives definition when $q=1$. The case $0<q<1$ seems to be particularly important (Yu et al., 2009). For simplicity and without loss of generality, in the following, we assume that: $t_0=0$, $0<q<1$.

In this section, we used the techniques of fractional calculus to analyze the behavior of the system (8) with squeeze film damping ($-\frac{p}{(a+x_1)^3}x_2$) with a fractional order:

$$\begin{aligned}
&\frac{d^{q_1}u_1}{dT^{q_1}}=x_2\\
&\frac{d^{q_2}x_2}{dT^{q_2}}=-rx_2-bx_1-cx_1^{\,3}-\frac{d}{(a+x_1)^2}+\frac{e}{(a+x_1)^8}+g\cos\Omega\tau-\frac{p}{(a+x_1)^3}\frac{d^{q_2}x_3}{dT^{q_3}}\\
&\frac{d^{q_3}x_3}{dT^{q_3}}=x_2
\end{aligned} \tag{10}$$

where, $0<q_1,q_2,q_3\leq 1$. Its order is denoted by $q=(q_1,q_2,q_3)$ here.

4.2. The 0-1 Test

The 0-1 test, proposed by Gottwald and Melbourne, (2004; 2005) is directly applied to the time series data, based on the statistical properties of a single coordinate (here in the variable x_1) (see Eq. 10). Basically, the 0-1 test consists of estimating a single parameter *K*. The test considers a system variable x_j, where two new coordinates (*p*,*q*) are defined as follows

$$p(n,\bar{c})=\sum_{j=0}^{n}x(j)\cos(j\bar{c}) \tag{11}$$

$$q(n,\bar{c})=\sum_{j=0}^{n}x(j)\sin(j\bar{c}) \tag{12}$$

where, $\bar{c}\in(0,\pi)$ is a constant. The mean square displacement of the new variables $p(n,\bar{c})$ and $q(n,\bar{c})$ is given by

$$M(n,c)=\lim_{n\to\infty}\frac{1}{N}\sum_{j=1}^{N}\left[(p(j+n,\bar{c})-p(j,\bar{c}))^2+(q(j+n,\bar{c})-q(j,\bar{c}))^2\right] \tag{13}$$

where $n=1,2,\ldots,N$ and, therefore, we obtain the parameter K_c in the limit of a very long time

$$K_c=\frac{\operatorname{cov}(Y,M(\bar{c}))}{\sqrt{\operatorname{var}(Y)\operatorname{var}(M(\bar{c}))}} \tag{14}$$

where vectors $M(\bar{c})=\left[M(1,\bar{c}),M(2,\bar{c}),\ldots,M(n_{\max},\bar{c})\right]$ and $Y=[1,2,\ldots,n_{\max}]$.

Given any two vectors x and y, the covariance $\operatorname{cov}(x,y)$ and variance $\operatorname{var}(x)$, of $n_{\max}$ elements, are usually defined as (Litak et al., 2013):

$$\operatorname{cov}(x,y)=\frac{1}{n_{\max}}\sum_{n=1}^{n_{\max}}\left(x(n)-\bar{x}\right)\left(y(n)-\bar{y}\right) \tag{15}$$

$$\operatorname{var}(x)=\operatorname{cov}(x,x) \tag{16}$$

where $\bar{x}$ and $\bar{y}$ are the average of $x(n)$ and $y(n)$, respectively. As a final result, the value of the searched parameter K is obtained taking the median of 100 different values of the parameter $\bar{c} \in (0, \pi)$ in Eq. (14). If the K_c value is close to 0 the system is periodic, on the other hand, if K_c value is close to 1 the system is chaotic. In all simulations we have chosen $n = 10000$ and $j = \frac{n}{100}, \ldots, \frac{n}{10}$.

4.3. Numerical Results and Discussions

Considering the numerical values for the parameters: $\Omega = 1$, $r = 0.1$, $b = 0.05$, $c = 0.35$, $d = 4/27$, $e = 0.0001$, $g = 0.2$, $p = 0.005$, $a = 1.6$, $x_{1_0} = 0$ and $x_{2_0} = 0$. Figure 8 shows the K variation for the derivate order for $q_1 = q_2 = 1$ and $0.5 \le q_3 \le 1$. It is possible to see that the behaviour of the chaotic system does not change with the variation of the order q_3, which represents the viscoelastic behavior of the squeeze film damping. However, note that when $q_3 < 1$, the value of K are higher (for $q_3 = 0.53$ we have K=0.9945, for $q_3 = 1$ we have K=0.9818), which indicates a change in chaotic behavior and a higher level is it.

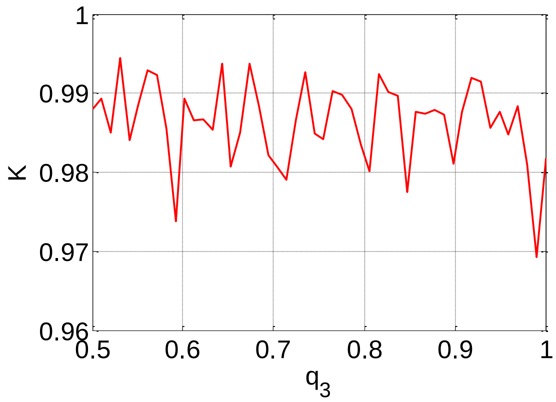

Figure 8. Variation of the K vs variation of the $0.5 \le q_3 \le 1$.

The displacement and the phase plane for ($q_1 = q_2 = 1$ and $q_3 = 0.53$) case can be observed in Fig. 9. They show that, to $q_3 = 0.53$, the system remains chaotic with a small increase in the displacement of the tip of the beam, which can be seen in Fig. 10.

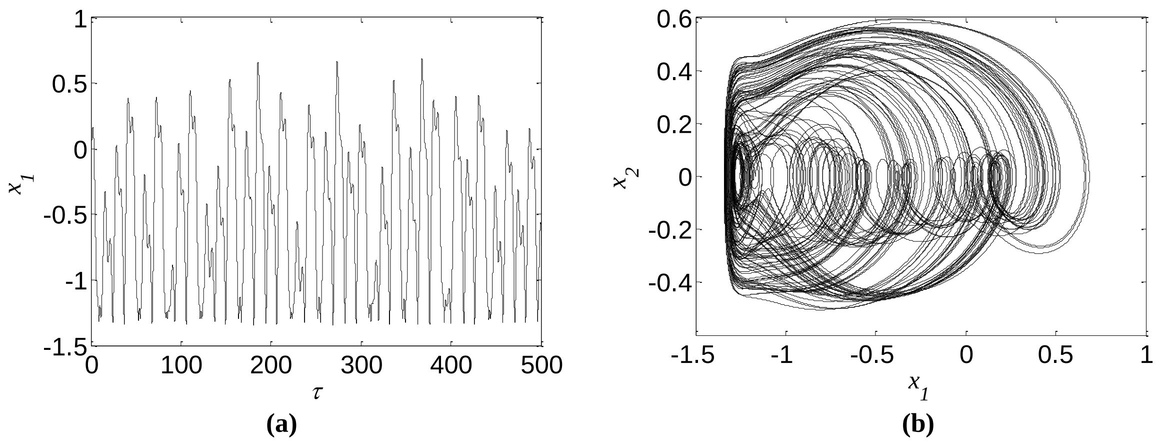

Figure 9. (a) Time history of the displacement of the tip. (b) Phase plane.

In Fig. 10, it is possible to observe a small increase in displacement of the tip of the beam, demonstrating the importance of analysis of the viscoelastic behavior of the surface of the sample.

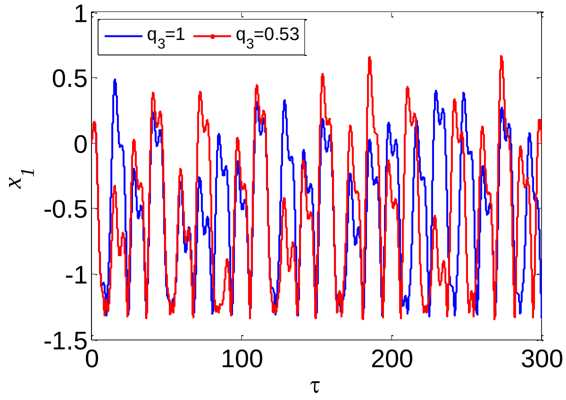

Figure 10. Time history of the displacement of the tip for ($q_1 = q_2 = 1$ and $q_3 = 1$ and $q_3 = 0.53$) case.

5. CONCLUSIONS

In this work, the nonlinear dynamics of an Atomic Force Microscope micro cantilever operating in tapping mode considering the influence of the damping, nonlinear stiffness term, and squeeze film damping in fractional-order, was investigated. Through numerical simulations it was possible to analyze the nonlinear dynamics of an AFM system.

The numerical results showed that the analyzed parameters play an important role because they can lead to different responses, like periodic and chaotic motion. In particular, for squeeze film damping in fractional-order, the results showed the influence of the order of the derivative on the displacement of the tip of the beam. The 0-1 test proved to be a good tool to characterize fractional-order differential systems.

6. ACKNOWLEDGEMENTS

The authors thank CAPES, FAPESP and CNPQ (proc: 447539/2014-0).

7. REFERENCES

Bagley, R. and Calico, R., 1991, "Fractional order state equations for the control of viscoelastically damped structures. J Guid Contr Dyn", pp. 14:304–11.

Balthazar, J. M., Bueno, A. M., Tusset, A. M. and Pontes, B. R. 2012a, "On an Overview of Nonlinear and Chaotic Behavior and Their Controls of an Atomic Force Microscopy (AFM) Vibrating Problem", In: Iva Lipovic. (Org.). Nonlinearity, Bifurcation and Chaos - Theory and Applications. 1ed.: InTech, Vol. 1, pp. 45-68.

Balthazar, J. M, Pontes, B.R., Tusset, A. M., Bueno, A. M. Felix, J. L. P., Nozaki, R., Rodrigues, K. S. and Iliuk, I., 2012b, "Progressos recentes em NEMS: Comportamento dinâmico não-linear e caótico e de possível controle da microscopia de força atômica ('AFM'), por meio de microvigas em balanço e uma breve discussão sobre colheita de energia para dispositivos baseados em MEMS", In: Carlos Graeff. (Org.). "Nanotecnologia: ciência e engenharia", Ed. Cultura Acadêmica, São Paulo, Brazil, Vol. 1, pp. 201-276.

Balthazar, J. M., Tusset, A. M. and Bueno, A. M., 2014, "Nonlinear TM-AFM control considering parametric errors in the control signal evaluation", Journal of Theoretical and Applied Mechanics (Warsaw), Vol. 52, pp. 93-106, 2014.

Burgess, W. and Daniel S., 2006, "Chaos affects atomic force microscopes", Photon Spectra, Vol. 40, pp. 101–102 .

Basso, M. and Bagni, G., 2004, "Controller synthesis for stabilizing oscillations in tapping-mode atomic force microscopes", IEEE Int Sympos Comput Aid Control Sys Design, pp. 372–377.

Frétigny, C. 2007. "Atomic Force Microscopy", Nanoscience Part I, pp. 91-119.

Garcia, R. and Pérez, R., 2002, "Dynamic atomic force microscopy method", Surface Science Report, Vol. 47, pp. 197-301.

Gottwald, G. and Melbourne, I., 2004. "A new test for chaos in deterministic systems", Proceedings of the Royal Society of London A, Vol. 460, pp. 603-611.

Gottwald, G. and Melbourne, I., 2005, "Testing for chaos in deterministic systems with noise", Physica D, Vol. 212, pp. 100-110.

Jalili, N. and Laxminarayana, K., 2004, "A review of atomic force microscopy imaging systems: application to molecular metrology and biological sciences", Mechatronics, Vol. 14, pp. 907-945.

Litak, G., Bernardini, D., Syta, A., Rega, G. and Rysak, A., 2013, "Analysis of chaotic non-isothermal solutions of thermomechanical shape memory oscillators", Eur. Phys. J. Special Topics, Vol. 222, pp. 1637-1647.

Nozaki, R., Balthazar, J. M., Tusset, A. M., Pontes, B. R. and Bueno, A. M., 2013, "Nonlinear Control System Applied to Atomic Force Microscope Including Parametric Errors", Journal of Control, Automation and Electrical Systems, Vol. 24, pp. 223-231.

Rodrigues, K. S., Balthazar, J. M., Tusset, A. M., Pontes, B. R. and Bueno, A. M., 2014, "Preventing Chaotic Motion in Tapping-Mode Atomic Force Microscope", Journal of Control, Automation and Electrical Systems, Vol. 25, pp. 732-740, 2014.

Yu, Y., Li, H.X., Wang, S. and Yu, J., (2009), "Dynamic analysis of a fractional-order Lorenz chaotic system", Chaos, Solitons and Fractals, Vol, 42, pp. 1181-1189.

Rutzel, S., Lee, S. I. and Raman, A., 2003, "Nonlinear dynamics of atomic-force-microscope probes driven is Lennard-Jones potentials", Proc. R. Soc. Lond, Vol. 459, pp. 1925-1948.

Zhang, W. M., Meng, G., Zhou, J. B. and Chen, J. Y., 2009, "Nonlinear Dynamics and Chaos of Microcantilever-Based TM-AFMs with Squeeze Film Damping Effects", Sensors, Vol. 9, pp. 3854-3874.

8. AUTHORIAL RESPONSIBILITY

"The authors are solely responsible for the content of this work".